PREDICTIONS OF THE FLOW FIELD AROUND SHIPS IN SHALLOW WATER BASED ON THE 2D–POTENTIAL THEORY

Laila Kamar
Ship Engineering Department, Faculty of Engineering and Technology,
Suez-Canal University, Port Said, Egypt.

ABSTRACT

In many practical applications, engineers are concerned with predicting flows around ships. Thereby, hydrodynamic characteristics, as well as, the resistance behaviour can be assessed. The paper presents a fast calculation method based on the two-dimensional potential theory which here is applied for the first time to real ship bodies floating in shallow water (h/T = 1.2 to 2.5). The advantages and restrictions of application of this procedure are discussed. In addition, the computed velocities are compared with experimental data measured in model tests. It is remarkable, that the computed and the measured data do well agree even in the case of extreme shallow water (h/T = 1.2).

Keywords: Potential Flow, Shallow Water, Body of Revolution, Velocity Distribution around Ship Hulls, Calculation of Additional Velocities

Nomenclature

A	local cross-sectional area
A_M	midship section area
B	breadth of ship or ship model
C_P	prismatic coefficient, C_P = Volume of displacement / $(L_{WL}.A_M)$
D	diameter/breadth of the axi-symmetrical body
F_n	Froude number, $F_n = U_0 / (L_{WL}.g)^{1/2}$
F_{nh}	Froude depth number, $F_{nh} = U_0 / (h.g)^{1/2}$
g	acceleration of gravity
h	water depth
K_B	breadth correction factor
$L'/2$	length of the dipole distribution of fore or after body
L_{WL}	length of water line
n	actual number of image
r	radial coordinate, $r^2 = y^2 + z^2$
T	draft
U_0	speed of ship or model
x	longitudinal coordinate related to $L_{WL}/2$
x'	longitudinal coordinate related to $L'/2$
y	lateral coordinate related to D/2
z	coordinate normal to the water surface related to D/2
β	integration variable in x-direction related to $L'/2$
Ψ	stream function
$\mu(x')$	dipole strength distribution, proportional to sectional area curve
$\mu^*(x')$	corrected dipole strength distribution
$s(x')$	dimensionless source / sink distribution, $s = -d\mu/dx'$

subscripts

a, f	after body and fore body
C	calculation
E	experiment
$\Psi = 0$	determined for $\Psi = 0$

1. INTRODUCTION

The flow field around ships and the deformation of the free water surface undergo growing changes with decreasing water depth. As a result, the additional velocities increase and the stimulation of waves is intensified. Consequently, the ship resistance and the required power rise. The resistance behaviour is usually investigated in the frame of model tests at different

water depths. The experimental results then are transfered to the large scale ship. However, because of the considerable cost of experiments the availability of numerical prediction methods is desirable.

The three-dimensional flow field can be described by the Navier Stokes equations and additional equations to account for the turbulent flow properties, see e. g. [1]. The numerical solution of the system of differential equations leads to the distributions of all involved field variables. The 3D–potential theory, e. g. [2], is able to determine the flow field, too. Though, turbulent flow behaviour and flow separation are not considered. In principle, both methods allow a good approximation of the real conditions of ship hulls. But applications need extensive efforts in defining the computational grid system. Moreover, the iterative solutions can be carried out only on large and fast computers.

An easy and fast tool for flow field calculations is given by the 2D-potential theory with axially distributed sources and sinks. The fluid viscosity and turbulent flow properties are neglected as in the 3D–potential theory. Moreover, deformations of the free surface are excluded in the present study. Although the 2D–theory represents generally an approximation, this method has been successfully applied in various works. In detail, these are applications to simple analytical hulls with identical fore and after body floating in deep water [3], [4] as well as in shallow water [5], [6]. A comparison of computed and measured data was performed, but only for a parabolized slender body [5]. An application to a simple asymmetrical hull with different fore and after body [7] was conducted only for the case of deep water without any comparison with experimental results.

The present paper outlines an extension of the theory and its application to real ship hulls with asymmetrical forms floating in shallow water. The considerations are related to seagoing ships and their models, for which measured velocities have been published. The computational and experimental results will be compared. Furthermore, the applicability of this procedure will be investigated especially in the case of shallow water.

2. THEORETICAL BACKGROUND

Under the above mentioned assumptions, the 2D-potential theory is valid for an axially symmetrical body floating in unrestricted water. The flow around the body is described by superposing the translational undisturbed flow and the flow produced by a continuous distribution of sources / sinks or of dipoles on the longitudinal axis. The formulation results in an equation for the stream function which allows the calculation of radial and axial velocity components by differentiating this equation (3). The streamline $\Psi = 0$ represents the hull contour of the body produced according to the potential theory. The comparison of the modelized contour with the one of the original body reveals a deformation. This can partly be compensated by introducing the breadth correction factor K_B as a multiplier of the dipole distribution and by extending the latter over an adjusted length L′. In order to use the concept also in the case of restricted water depth, the method of images will be incorporated [8], whereby the 3D–character of the flow field is taken into account. The application to ship forms needs a replacement of the cross-sectional areas by semicircular cross sections with equal areas. When considering simple ship forms with identical contours of fore and after body, quite plausible, useful results can be obtained [3], [5].

In the current study the theory will be extended to cover the real ship hull conditions. The calculation is based for that purpose on the assumption that the fore and the after body are of the same length $L_{WL}/2$ but of course of different hull contours. Accordingly, two separate dipole distributions μ_f (fore) and μ_a (after) ranging over the modified lengths $L'^f/2$ and $L'^a/2$ will be introduced. Because both parts meet amidship (x = 0) the same area, the breadth correction is identical for both sides. Finally, the equation for the stream function at any given point x, y, z within the flow can be derived as

$$\Psi = \pi . U_o . \left(r . \frac{D}{2}\right)^2 . \left[1 - \frac{K_B}{2} . \sum_{n=-\infty}^{n=+\infty} \left(\frac{D}{L_a'}\right)^2 . \int_{-1}^{0} \frac{\mu_a . d\beta}{N_a} + \left(\frac{D}{L_f'}\right)^2 . \int_{0}^{+1} \frac{\mu_f . d\beta}{N_f}\right] \quad (1)$$

with the denominators N_a and N_f, respectively

$$N_{a,f} = [(X'_{af} - \beta)^2 + (z_n^2 + y^2) / (L'_{a,f}/D)^2]^{3/2}$$

The subscript n indicates the running number of the actual image in z–direction and $z_n = z + (2nh) / (D/2)$ the actual distance of the imaged point.

The local velocity in x-direction follows from

$$\frac{U_x}{U_o} = \frac{1}{2.\pi.U_o.r.\left(\frac{D}{2}\right)^2} \cdot \frac{\partial \Psi}{\partial r} \qquad (2)$$

When using source/sink distributions, the equation for the dimensionless additional velocity results in

$$\frac{U_x}{U_o} - 1 = -\frac{K_B}{4} \cdot \sum_{n=-\infty}^{n+\infty} \left(\frac{D}{L_a'}\right)^2 \cdot \int_{-1}^{0} \frac{\sigma.(x_a' - \beta).d\beta}{N_a} + \left(\frac{D}{L_f'}\right)^2 \cdot \int_{0}^{+1} \frac{\sigma.(X_f' - \beta).d\beta}{N_f} \qquad (3)$$

In the strict sense, the modified length L'_a and L'_f and the breadth correction factor K_B must be adjusted separately for each considered dipole distribution. The length ratios L'_a / L_{WL} and L'_f / L_{WL} lie generally close to one and small deviations entail only insignificant errors. Therefore, in order to simplify a wellknown analytical formula for the ellipsoid of revolution [5] is used. The breadth correction factor K_B will always be determined before computing the velocities for the considered case according to the procedure cited in [6]. As equation (3) indicates, the dimensionless velocity components resulting from the simple potential theory show no dependency on the absolute speed U_0.

3. INVESTIGATED MODELS AND TEST CONDITIONS

The computations will be carried out for three models of seagoing ships with prismatic coefficients C_P of 0.6, 0.7 and 0.8. These models have been towed at the water depth / draft ratios of h/T = 1.2, 1.5 and 2.5. Different speeds have been realized in such a manner that the range of the Froude depth number is $F_{nh} < 1$ [9]. The model data and the upper limits of F_n and F_{nh} in the tests are listed in table . The breadth of the towing tank was about 10 m.

Measured local velocities along a line parallel to the longitudinal axis (y = const., z = 0) are available from the tests. Furthermore, the mean additional velocities have been determined by averaging the local values over the range $-1 \leq x \leq 1$. Both, the local and the mean data will be used here for comparison. The experimental data indicate that strong waves occur on the free surface for $F_{nh} > 0.55$. As already known [5], [8], such conditions cannot be treated with the present method and the affected cases will be left out of consideration.

4. NUMERICAL SIMULATION AND RESULTS

In order to apply arbitrary dipole distributions, all evaluations of the equations (1) to (3) will be carried out numerically. According to the investigation in [6], the number of images can be restricted for practical applications. The present cases need no more than n = 70 images.

Following the idea explained in [10], the dipole distribution for axially symmetrical bodies can be put up proportionally to the dimensionless cross sectional area A/A_M. The latter are represented separately for the fore and the after body by polynomials of higher order, which meet amidship the conditions $\mu_a = \mu_f = 1$ and $d\mu_{a,f} / dx = 0$. Figure (1) illustrates exemplarily for model No 1, that such polynomials (dashed line) sufficiently constitute the given cross–sectional area data.

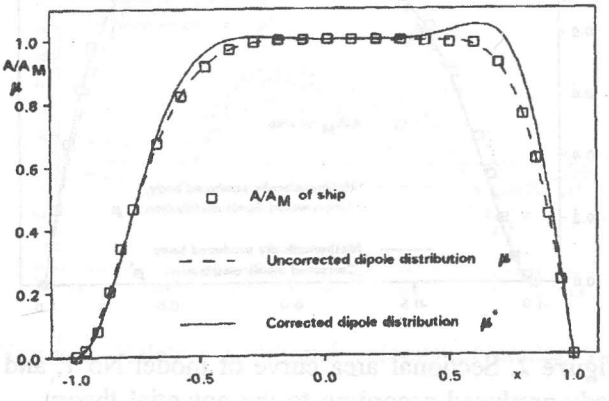

Figure 1. Sectional area curve and dipole distribution of model No 1.

According to the potential theory, the streamline $\Psi = 0$ describes the hull of the body. The radius and cross sections $(A/A_M)_{Y=0}$ of this synthetical body can be determined on deep water from equation (1) by iteration. Figure (2) compares this contour (dashed line) with the original cross-sectional areas again in the case of model No 1. In spite of breadth and length correction, appreciable deviations appear near stem and stern and, above all in the ranges $-0.7 < x < -0.2$ and $0.2 < x < 0.8$, respectively.

Table 1. Data of the ship models and of the mathematical bodies.

Data of the ship models and investigated Froude-Number ranges							Data of bodies of revolution		
Model Scale	L_{WL} [m]	B [m]	T [m]	C_P [-]	F_n ≤	F_{nh} ≤	D [m]	C_P 1)	C_P 2)
No 1 1:40	5.438	0.731	0.298	0.794	0.20	0.60	0.742	0.769	0.790
No 2 1:25	5.576	0.762	0.324	0.701	0.26	0.66	0.787	0.698	0.707
No 3 1:30	5.289	0.817	0.325	0.599	0.24	0.65	0.813	0.619	0.609

1) potential theory (Y = 0), uncorrected dipole distribution μ
2) potential theory (Y = 0), corrected dipole distribution μ^*

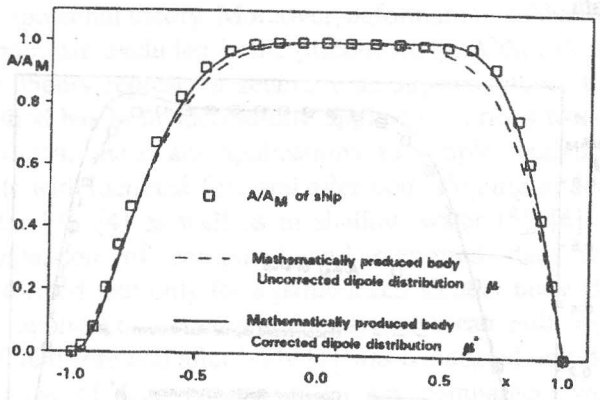

Figure 2. Sectional area curve of model No 1, and its body produced according to the potential theory.

In order to achieve an improved reproduction, new polynomials μ^* are derived from modified cross–sectional areas

$$\left(\frac{A}{A_M}\right)^* = \left(\frac{A}{A_M}\right) \cdot \left[\frac{A/A_M}{(A/A_M)_{Y=0}}\right]$$

The corrected dipole distributions of model No 1 show partly values $\mu^* > 1$, see Figure (1). But as Figure (2) demonstrates, these distributions produce a considerably better hull contour.

A further comparison examines the volumes of displacement and the prismatic coefficients. The data of the theoretical bodies are calculated by volume integrals over the cross sections and are listed in the right part of Table (1). While the use of uncorrected dipole distributions results in up to 3.3% smaller volumes, the volumes in the corrected cases differ less than 1.7% from the ship data.

As the cross sections of the ship models are converted into half circles within the proposed theory, conflicts arise amidship concerning the ground clearance in case of extreme shallow water. Therefore, the calculations cannot be based on the experimental water depth. In order to carry out the calculations with proper water depth conditions, the following two proposals will be investigated.

Proposal 1: $h_C - T_C = h_E - T_E = \text{const.}$
Proposal 2: $h_C / T_C = h_E / T_E = \text{const.}$

with $T_C = D/2$. The position y = const. of the computed velocities will be shifted also for geometrical reasons for the produced body. Thereby, the absolute distance between this line and the outside surface of the half circle at the middle of the body corresponds to the distance in the tests.

Figures (3) to (7) examplarily display predicted and measured additional velocities $(U_x - U_0) / U_0$ in

respective legends.

The Figures (3) and (4) show results of the models No 1 and No 2 for h/T = 1.2. They also include computed data in the case of an uncorrected dipole distribution. It is evident, that the extreme values are more accurately represented by the corrected distribution. In deeper water and at any floating condition in case of the model No 3 with the lowest C_P, the differences between the two calculation modes are smaller.

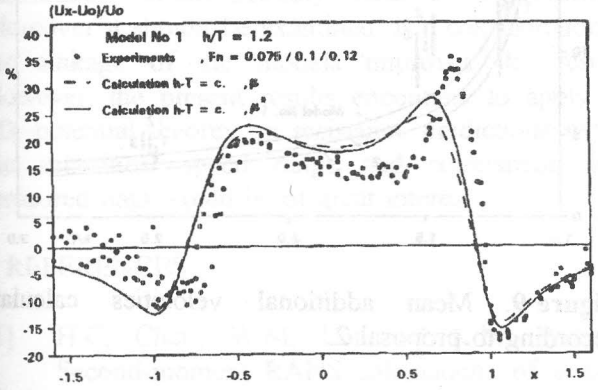

Figure 3. Relative additional velocity percentages. (The calculation is based on proposal 1).

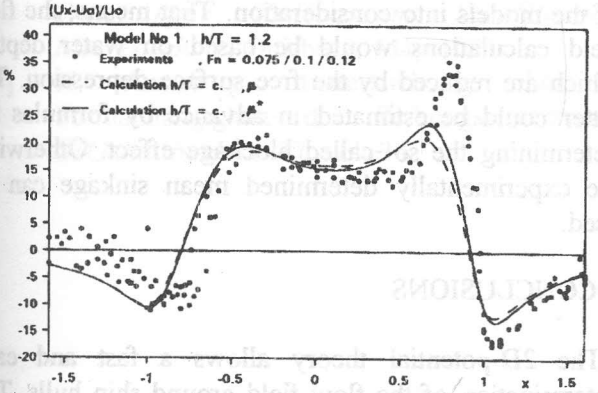

Figure 4. Relative additional velocity percentages. (The calculation is based on proposal 2).

The test results imply within the considered Froude–number ranges an influence of the speed. An increase of U_0 results in more pronounced peaks on the fore body, in deeper minima at stem (x = 1) and stern (x = −1) and in intensified fluctuations with changing sign of U_x–U_0. As already mentioned, the presented theory comprises no dependency on U_0. Therefore, the computed data always show continuous curves which approach asymptotically the abscissa for x > 1 and x < −1. It is obvious that the calculated velocities agree best with the test results at minimum speed.

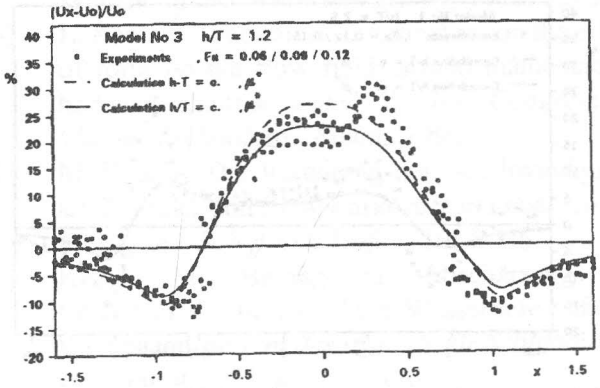

Figure 5. Relative additional velocity percentages.

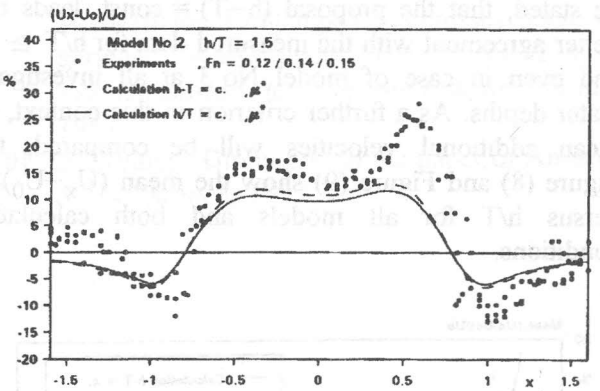

Figure 6. Relative additional velocity percentages.

The computed maxima on the fore body of model No 1 and No 2 lie somewhat closer to the midship section. They are less towering than the peaks in the experiments, in particular for h/T ≥ 1.5. In contrast to the models No 1 and No 2, model No 3 has no parallel middle body. Therefore, the curves computed for model No 3 show no pronounced maxima, see Figure (5). The theory correctly represents the minima around stem and stern for h/T = 1.2. But the positions near the stern lie at smaller x than in the tests. Similar to the maxima, the computed minima are less pronounced in cases of h/T ≥ 1.5, see Figures (1) and (2). It would be of interest to examine if refined dipole distributions

reproduce the original cross section areas more accurately as shown in the Figures and and if they yield a closer agreement with the experimental velocities.

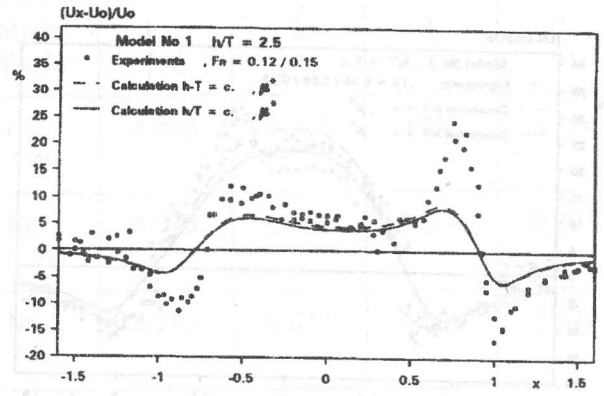

Figure 7. Relative additional velocity percentages.

Concerning the transfer rule of the water depth it can be stated, that the proposal (h–T) = const. leads to a better agreement with the measured data for h/T $\geq$ 1.5 and even in case of model No 3 at all investigated water depths. As a further criterion in this context, the mean additional velocities will be compared, too. Figure (8) and Figure (9) show the mean $(U_x-U_0)/U_0$ versus h/T for all models and both calculation conditions.

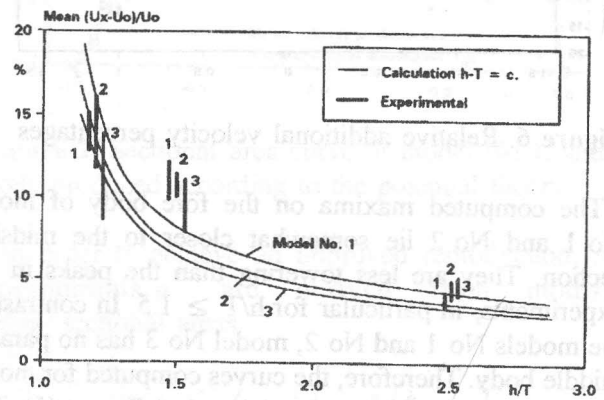

Figure 8. Mean additional velocities calculated according to proposal 1.

The curves provide information about the resistance increase in shallow water. The experimental data are plotted as bars representing their U_0–dependence. It is noteworthy, that the computed results agree very well with the test data for h/T = 1.2 and h/T = 2.5. Though, the test data for h/T = 1.5 lie considerably higher and form together with the other data an almost linear dependence on h/T. This effect may be due to interactions of the boundary layers at the bottom of the model and at the canal bed.

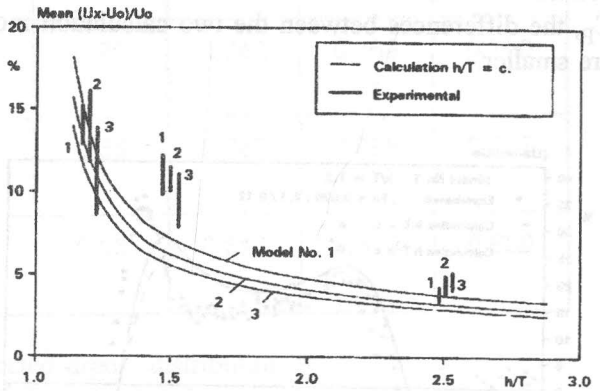

Figure 9. Mean additional velocities calculated according to proposal 2.

When comparing both Figures, no further understanding can be found concerning the water depth–transfer proposal. Within a next step of investigations it would be of interest to take the sinkage of the models into consideration. That means, the flow field calculations would be based on water depths, which are reduced by the free surface depression. The latter could be estimated in advance by formulas for determining the so–called blockage effect. Otherwise, the experimentally determined mean sinkage can be used.

5 CONCLUSIONS

The 2D-potential theory allows a fast and easy determination of the flow field around ship hulls. The velocity components can be predicted seperately at any point without knowledge of the complete flow. As pointed out, this theory is only applicable at low F_{nh}–numbers. In the present cases, the determined local flow velocities agree sufficiently with the test results, even in extreme shallow water h/T = 1.2.

The approximation of the ship hulls by bodies of revolution leads to certain restrictions. On the one hand, there is an uncertainty concerning the suitable water

depth for the prediction, whereas on the other hand, there are extreme local additional velocities which are somewhat underpredictable. In the cases considered here, this can be seen around the stem and the stern and in the region of the maxima on the forebody.

When taking into account the mean additional velocities, the above mentioned local differences play only a secondary role. Apart from the discrepancy for h/T = 1.5, the calculated and the experimental data do well agree.

A more sophisticated formulation of the dipole distribution would possibly yield an improvement. Moreover it should be examined, if a consideration of the sinkage of the models improves the results. However, the present results encourage to apply the 2D–potential theorey on resistance predictions within the subcritical speed range and comparison with measured data would be of great interest.

6 REFERENCES

[1] H.C. Chen, W.M. Lin and K.M. Weems,: Second-moment RANS calculations of viscous flow around ship hulls *Proc. CFD Workshop*, vol. 1, Ship Research Institute, Tokyo, 1994.

[2] G. Jensen, A. Cura Hochbaum,: Einfluß der Wassertiefe auf die Hinterschiffsumströmung *15. Duisburger Kolloquium Schifftechnik/ Meerestechnik*, Duisburg, May 1994.

[3] H. Amtsberg,: Untersuchung über die Formabhängigkeit des Reibungswiderstandes *STG-Jahrbuch*, 1937, vol. 38.

[4] M. Kirsch,: Die Erzeugung von Rotationskörper aus vorgegebenen Singularitäten *Schiff und Hafen*, 1959, No 11.

[5] W. Grollius,: Untersuchung des Strömungsfeldes analytischer Schiffsformen auf flachem Wasser im Geschwindigkeitsbereich geringer Wellenbildung *Schiff und Hafen*, 1975, No 9.

[6] L. Kamar,: Theoretical investigation on the effect of form on the flow field around mathematical bodiesin shallow water *5th Int. Congress of Marine Technology*, Athens 1990.

[7] M. Kirsch,: Die Verteilung der Geschwindigkeit am Zylinder und Rotationskörper in unbegrenzter Flüssigkeit *Schiff und Hafen*, 1962, No 11.

[8] Kirsch, M.: Beitrag zur Abschätzung des Einflusses der beschränkten Wassertiefe auf den Widerstand *Bericht des Instituts für Schiffbau der Universität Hamburg*, No 133.

[9] H. Binek,: Modellmäßige Widerstands- und Propulsionsuntersuchungen von Seeschiffsformen unter systematischer Veränderung des Wassertiefen-Tiefgangs-Verhältnisses bis zu sehr geringen Wassertiefen *Bericht No 1236 der Versuchsanstalt für Binnenschiffbau Duisburg*, 1989.

[10] F. Weinig,: Discussion to the paper of Amtsberg *STG-Jahrbuch*, 1937, vol. 38.